# A semiconductor-based, frequency-stabilized mode-locked laser using a phase modulator and an intracavity etalon

**Josue Davila-Rodriguez,[1,*] Ibrahim Ozdur,[1] Charles Williams,[1] and Peter J. Delfyett[1,2]**

[1]*CREOL, The College of Optics and Photonics, University of Central Florida, 4000 Central Florida Blvd., Orlando, Florida 32816-2700, USA*

[2]*E-mail: delfyett@creol.ucf.edu*

**Corresponding author: josue@creol.ucf.edu*

Received July 21, 2010; revised November 2, 2010; accepted November 12, 2010; posted November 15, 2010 (Doc. ID 131968); published December 9, 2010

We report a frequency-stabilized semiconductor-based mode-locked laser that uses a phase modulator and an intracavity Fabry-Perot etalon for both active mode-locking and optical frequency stabilization. A twofold multiplication of the repetition frequency of the laser is inherently obtained in the process. The residual timing jitter of the mode-locked pulse train is 13 fs (1 Hz to 100 MHz), measured after regenerative frequency division of the photodetected pulse train. 

*OCIS codes:* 140.4050, 140.3425.

Mode-locked lasers as frequency comb sources with multigigahertz comb-line spacing and high-frequency stability are desirable for applications in coherent communications, signal processing, and optical arbitrary waveform generation [1,2]. Harmonically mode-locked lasers stabilized to an intracavity Fabry-Perot etalon (FPE) through a Pound–Drever–Hall (PDH) scheme have been demonstrated, producing multigigahertz spaced frequency combs with excellent frequency stability [3,4]. In these comb sources, the long fiber cavity provides narrow longitudinal mode linewidths, while the FPE sets the large mode-to-mode spacing.

The PDH stabilization loop typically requires an independent rf source in order to phase modulate a portion of the output optical comb and derive an error signal by probing the FPE resonance through a technique analogous to frequency modulation spectroscopy [5,6]. However, there is a trade-off between the optical power available as usable laser output, which is used in the stabilization loop and the output coupling ratio of the cavity. Since the slope of the error signal increases with optical power, using a larger fraction of the light in the stabilization loop results in a tighter lock, but this must be done at the expense of the available power in the output pulse train or by increasing the cavity output coupling, which reduces the laser's cavity quality factor.

Mode-locked lasers based on a combination of phase modulation and periodic spectral filtering have been demonstrated as a method of multiplying the repetition rate by using the higher-order sidebands generated from the phase modulation process [7,8].

In this work, a mode-locked laser is presented in which both mode-locking and frequency stabilization are achieved using a single phase modulator and the intracavity etalon. Using the same intracavity elements for both purposes achieves a simplification of the feedback loop that is typically used [4] and reduces the number of intracavity elements. It should be noted that in this setup (Fig. 1), all of the intracavity power is used for the stabilization loop, which is roughly an order of magnitude larger than the output power, creating tighter lock while avoiding the trade-off with the available power at the output. Also, the repetition rate of the output pulse train is twice that of the signal driving the phase modulator.

A commercially available semiconductor optical amplifier (SOA) is used as the gain medium, and the phase modulator is driven at exactly one-half the free-spectral range (FSR) of the FPE. The etalon is built with an ultralow expansion quartz spacer, is hermetically sealed to mitigate the effects of environmental fluctuations, and has an FSR = 10.285 GHz and a finesse of 1000. The fiber cavity is ~28 m long and is composed entirely of standard single-mode fiber. Mode locking is attained by the combination of high-depth phase modulation (~1.85 to 2 rad) and the periodic spectral filtering provided by the etalon. The diagram in Fig. 2 shows the phase modulation sidebands generated by the phase modulator and the transmission function of the FPE. Only the modes within the etalon transmission peaks are allowed to oscillate and become part of the mode-locked spectrum. Note that the transmitted modes are in phase with the main carrier and spaced by twice the modulation frequency; therefore the amplitude of the transmitted field is modulated at the

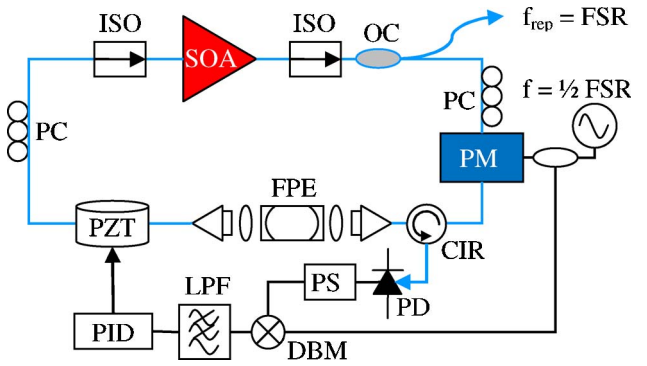


Fig. 1. (Color online) CIR, circulator; DBM, double balanced mixer; FPE, Fabry–Perot etalon; ISO, isolator; LPF, low-pass filter; OC, output coupler; PC, polarization controller; PD, photodetector; PID, proportional-integral-differential controller; PM, phase modulator; PS, phase shifter; PZT, piezoelectric transducer (fiber stretcher); SOA, semiconductor optical amplifier.

 

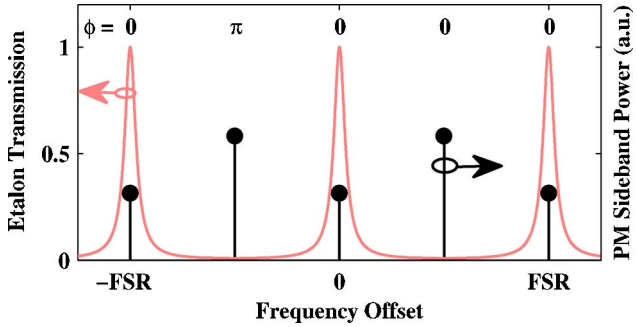


Fig. 2. (Color online) Phase modulation sidebands (black lines) and FPE transmission peaks (red lines). The mode locking occurs owing to the combination of phase modulation and periodic spectral filtering. The finesse of the cavity for this plot is $F = 100$, and the depth of modulation $\beta = 1.84$ rad, for illustration purposes.

FSR of the etalon. The reflected sidebands (together with a portion of the carrier when it is off resonance) are collected through a circulator and photodetected to generate a PDH error signal that is demodulated by mixing in quadrature with the driving signal. This signal is used to control the fiber cavity length via a piezoelectric fiber stretcher and keep the lasing frequency at the peak of the FPE transmission. The main advantages of the system simplification are the following: (1) the number of intracavity elements is reduced, reducing the footprint of the system and potentially leading to a cavity design with lower loss, (2) an additional rf oscillator is not needed for the stabilization loop, and (3) the useful output power is increased, since there is no need to use a portion of it in the stabilization loop.

The mode-locked laser output consists of a pulse train with 10.285 GHz repetition rate and average power of ~5 mW. The optical spectrum is a comb of optical frequencies spaced by 10.285 GHz and has a 10 dB bandwidth of ~3 nm [Fig. 3(a)]. A high resolution trace of one comb line is shown in Fig. 3(b). The observed optical signal-to-noise ratio is 60 dB at a resolution bandwidth of 1 MHz. No residual optical tones spaced by the driving frequency were observed in a high-resolution measurement with a noise floor at −45 dBc with a resolution bandwidth of 25 MHz. An average of 12 sampling oscilloscope traces of the corresponding pulse train is shown in Fig. 3(c), using an oscilloscope with an equivalent bandwidth of 30 GHz. Pulse autocorrelation traces are measured directly out of the laser and after compression in a dual grating compressor [Fig. 3(d)]. The autocorrelation width of the compressed pulse is <2 times the transform limited autocorrelation calculated from the optical spectrum.

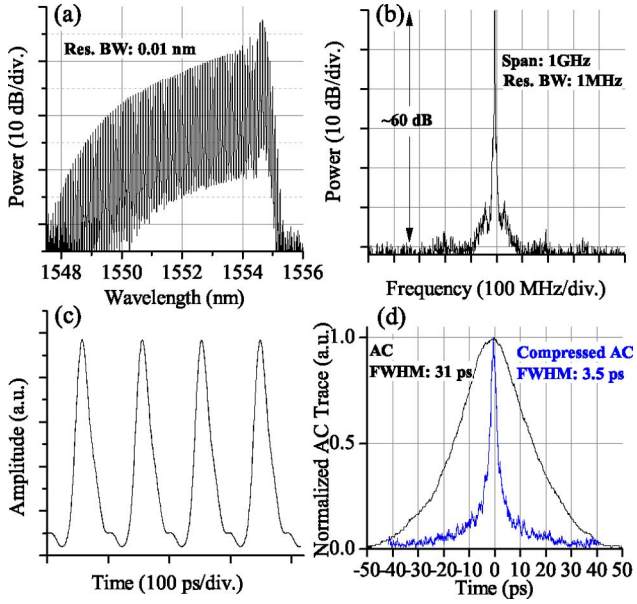


Fig. 3. (Color online) Mode-locked laser characteristics. (a) Optical spectrum, (b) high-resolution optical spectrum of a single comb line, (c) sampling oscilloscope trace of the photodetected pulse train, (d) mode-locked pulse autocorrelation trace.

Frequency stability and optical linewidth measurements are performed by heterodyning a relatively stable commercially available cw laser with one of the mode-locked spectrum comb lines and measuring the resulting radio-frequency beat note. A heterodyne beat note with FWHM of ~4 kHz is shown in Fig. 4 (top). A spectrogram was recorded over 40 s and is shown in Fig. 4 (bottom). The maximum frequency deviation in this time span is ~200 kHz. This measurement is ultimately limited by the stability of the cw laser.

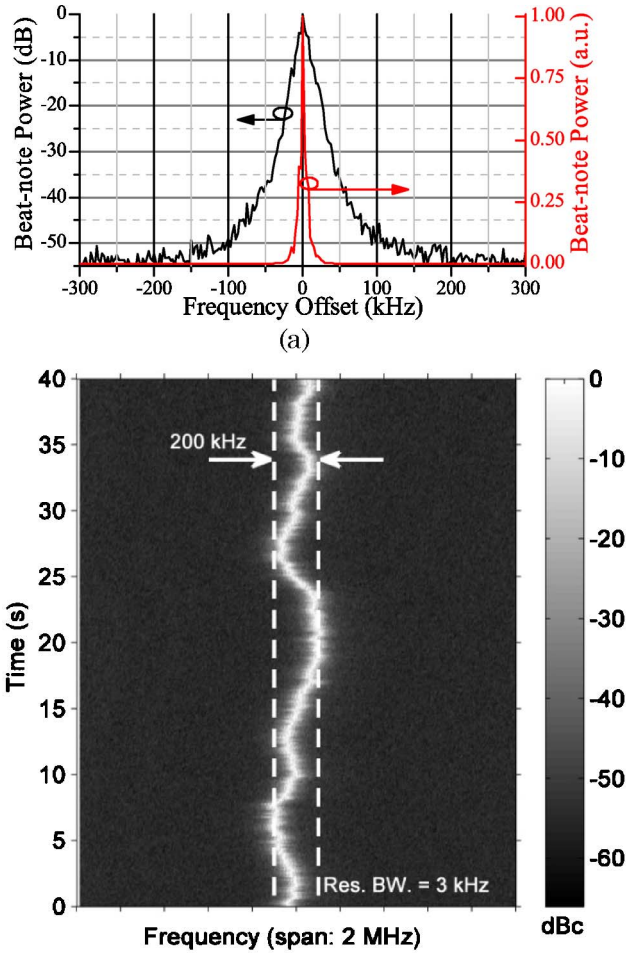


Fig. 4. (Color online) Heterodyne beat between one mode-locked laser comb line and a cw laser (top) and 40 s spectrogram of the heterodyne beat (bottom).

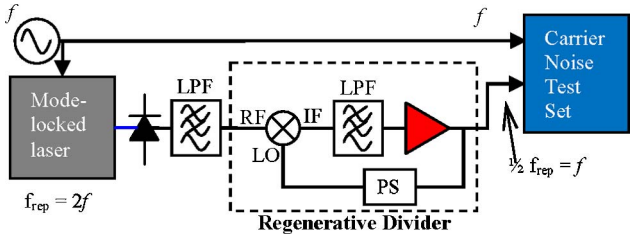


Fig. 5. (Color online) Phase-noise measurement setup.

Measuring the residual timing jitter on the pulse train is a more challenging problem, since the repetition rate of the pulse train is twice that of the driving source. For this reason, a regenerative frequency divider (Fig. 5) was designed and used for the measurement.

The resulting measurement is the residual jitter of both the mode-locked laser and the regenerative divider. Theory for regenerative division states that a perfect regenerative divider decreases the phase-noise power-spectral density (PSD) by a factor of 4 (−6 dB), which preserves the rms timing jitter of the original signal [9]. The results presented here show the noise PSD at 5.1425 GHz, and its integrated timing jitter, which is that of the 10.285 GHz signal plus a small amount added by random fluctuations in the frequency divider. Phase-noise measurement results are shown in Fig. 6. The rms timing jitter of the 10.285 GHz pulse train is calculated to be ~13 fs in the integration band from 1 Hz to 100 MHz.

In conclusion, a mode-locked laser is presented in which both mode locking and PDH locking to an intracavity FPE are achieved by using a single phase modulator. The output of the laser consists of a multigigahertz spaced frequency comb stabilized to the transmission peaks of the FPE. The comb lines exhibit a frequency instability <200 kHz over 40 s and an optical signal-to-noise ratio >60 dB, which makes this laser suitable for applications in arbitrary waveform generation, coherent communications, and photonic analog-to-digital conversion. A reduction of intracavity elements is achieved, which allows for a system with reduced footprint. The residual timing jitter of the system, including a necessary regenerative divider, is found to be 13 fs.

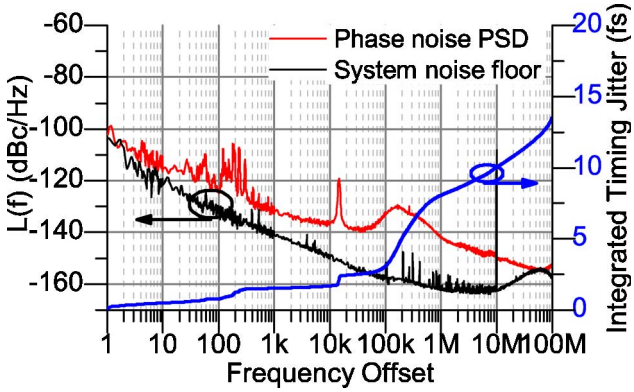


Fig. 6. (Color online) Phase-noise power spectral density of the frequency-divided rf tone and integrated timing jitter. The integrated timing jitter is the same as in the 10.285 GHz signal.

## References

1. P. J. Delfyett, S. Gee, M.-T. Choi, H. Izadpanah, W. Lee, S. Ozharar, F. Quinlan, and T. Yilmaz, J. Lightwave Technol. **24**, 2701 (2006).
2. Z. Jiang, D. E. Leaird, and A. M. Weiner, Opt. Express **13**, 10431 (2005).
3. F. Quinlan, S. Ozharar, S. Gee, and P. J. Delfyett, J. Opt. A **11**, 103001 (2009).
4. I. Ozdur, M. Akbulut, N. Hoghooghi, D. Mandridis, S. Ozharar, F. Quinlan, and P. J. Delfyett, IEEE Photonics Technol. Lett. **22**, 431 (2010).
5. E. D. Black, Am. J. Phys. **69**, 79 (2001).
6. R. W. P. Drever, J. L. Hall, F. V. Kowalski, J. Hough, G. M. Ford, A. J. Munley, and H. Ward, Appl. Phys. B **31**, 97 (1983).
7. K. S. Abedin, N. Onodera, and M. Hyodo, Appl. Phys. Lett. **73**, 1311 (1998).
8. K. S. Abedin, N. Onodera, and M. Hyodo, IEEE J. Quantum Electron. **35**, 875 (1999).
9. E. Rubiola, M. Olivier, and J. Groslambert, IEEE Trans. Instrum. Meas. **41**, 353 (1992).